ELSEVIER

International Journal of Pharmaceutics 246 (2002) 1–16

international journal of pharmaceutics

www.elsevier.com/locate/ijpharm

Heat transfer in vial lyophilization

M. Brülls [a], A. Rasmuson [b,*]

[a] AstraZeneca R&D Mölndal, SE-43183 Molndal, Sweden

[b] Chalmers University of Technology, Department of Chemical Engineering Design, SE–41296 Gothenburg, Sweden

Received 10 December 2001; accepted 10 June 2002

Abstract

Heat transfer in vial lyophilization has been studied experimentally and theoretically as a first step in developing a theoretical model for vial lyophilization. Heat transfer was studied by cooling and heating sealed vials containing water in a pilot scale freeze-dryer. The factors studied were bottom curvature of the vial, chamber pressure, fill volume, position on the shelf and the state of the water. A theoretical dynamic and two-dimensional axisymmetric model that comprised both the vial and its content was developed. It was constructed using physical models for thermal conductivity of gases at low pressure, thermal conduction and radiation. The coefficients in the model were based on physical constants and geometrical data and not assessed from experiments. The resulting differential equations were solved numerically. The theoretical model could well describe both heat transfer and heat accumulation in the vial. The dynamics of the corner vials could also be well modeled by adding heat transfer to the side of the vial. The effect of the curvature of the vial bottom, the heat accumulation in the glass vial and the heat transfer to the sidewalls of vials in the corner of the shelf all contributed to a significant radial influence on the heat transfer.

Keywords: Lyophilization; Freeze-drying; Vial; Heat transfer; Simulation; Mathematical model

1. Introduction

Of all pharmaceutical unit operations, drying processes contribute the most to the manufacturing cost. Lyophilization is the most expensive of all drying operations both in capital investment and in operating expense. The high cost and commercial value per production batch demands careful attention to process design and process control. Theoretical modeling studies have considerable potential to guide experimental studies, thereby decreasing development time and improving the possibilities to achieve an optimal and robust process design.

The heat input during the lyophilization process must be well controlled to insure that the product temperature does not become too high. The structure of the product deteriorates at too high temperatures and the final quality of the product becomes unacceptable. It is however also important to maximize the heat input in order to optimize the process efficiency. The shelf tempera-

* Corresponding author. Tel.: +46-31-7722940; fax: +46-31-814620

E-mail addresses: mikael.brulls@astrazeneca.com (M. Brülls), rasmus@kat.chalmers.se (A. Rasmuson).

0378-5173/02/$ - see front matter
PII: S0378-5173(02)00353-8

ture and chamber pressure controls the heat input and these parameters should therefore be set so that an optimum product temperature is obtained. In practice, the appropriate shelf temperature and chamber pressure conditions are often established empirically in a 'trial-and-error' approach.

Pikal (Pikal, 1985; Pikal et al., 1983, 1984) presented theoretical modeling and experimental studies on the thermal and mass transport resistances in the sublimation process of vial lyophilization. Primary drying was presented as a coupled heat and mass transfer problem and used a pseudo steady-state model with a moving planar boundary. A macroscopic balance was set up, where the heat flow was given by the product of the mass flow and the heat of sublimation. Other researchers (Ybema et al., 1995; Schoen et al., 1995; Rene et al., 1993) have constructed similar models. These one-dimensional models can however not describe the heat transfer accurately. The radial dimension of the container is comparable to the length dimension and radial effects will therefore be significant. These models are also not dynamic which means that heat accumulation effects are not being modeled. The weight of the vial is generally several times larger than the product in the vial and heat accumulation in the vial should therefore not be ignored.

Other researchers (Mascarenhas et al., 1997; Sheehan and Liapis, 1998) have presented dynamic two-dimensional axisymmetric vial lyophilization models. These models describe the heat transfer more accurately but these models do not model the heat accumulation in the glass vial either. The heat transfer from the shelf to the vial is in both models represented by an empirically determined heat transfer coefficient. This means that a heat transfer coefficient must be fitted or determined experimentally for the process conditions and type of vial that will be used and the underlying heat transport mechanisms are not described.

The objective of this study was to thoroughly study heat transfer in vial lyophilization experimentally and to model it theoretically as a first step in developing a theoretical model for vial lyophilization. The experiments were performed in such a way that the conditions for the heat transfer were the same as during a lyophilization process but without mass transfer or freezing taking place. The developed simulation model was validated by comparing simulated and experimental results. The heat transfer model will be a fundament for the further development of a vial lyophilization model.

2. Theory

2.1. Heat exchange between the vials and the surroundings

Heat is exchanged mainly between the glass vials and the stainless steel shelf on which the vials is loaded but also the walls in the freeze-dryer and the shelf above the vials is taking part in the heat exchange with the vials. The possible modes of heat exchange are heat conduction through the gas between the vial and the surroundings, thermal radiation and heat conduction by direct contact between the shelf and the vial.

The bottom of a vial has considerable curvature and there is therefore a gap between the vial and the shelf. Direct contact between the shelf and the vial was therefore assumed to be negligible and this heat transfer mode was not included in the model. This assumption seems reasonable because the area where the vial is in direct thermal contact with the shelf is very small. The heat exchange between the bottom of the vial and the shelf was therefore assumed to only take part by heat conduction through the gas in the gap and by thermal radiation.

The glass vial was well shielded from the shelf above by the rubber stopper and the cap that the vial was sealed with. The stopper and the plastic cover on the cap are relatively poor thermal conductors and have poor heat capacity characteristics and it was therefore assumed that the vial was perfectly insulated on the upper side. The stopper and cap were not included in the model.

A vial in the center of the shelf was completely surrounded by neighbors in a hexagonal array and therefore well shielded from heat exchange with the surroundings from the side. It was therefore assumed that the sidewall of such a vial was perfectly insulated. A vial in the corner of the

shelf was however not shielded by neighboring vials and it was assumed that heat was exchanged between the walls of the freeze-dryer and the vial and that it was evenly and axisymmetrically distributed along the side of the vial. The amount of heat exchange from the side for a corner vial and the corresponding heat transfer coefficient were evaluated from the experiments and not based on theoretical relations.

2.2. Heat conduction in gases at low pressure

The gas in the freeze-dryer consisted mainly of nitrogen because the air from the start of the process was exchanged through nitrogen injection during the pressure regulation.

It is customary to refer to four different regimes when heat conduction in gases at low pressures is considered. The regimes are distinguished by referring to the Knudsen number, which is the ratio of the mean free path of molecules to a characteristic length that is usually taken to be the width of the gas layer. The four different regimes are the continuum regime, temperature-jump regime, intermediate or transition regime and free molecule regime. Free molecular flow occurs when the mean free path is greater than the width of the gas layer, which in this case is the gap between the vial and the shelf. An approximate calculation of the mean free path (λ) can be made by the relation (Dushmann and Lafferty 1962):

$$\lambda = \frac{1}{\pi N d^2 \sqrt{2}} \simeq \frac{3.1 \times 10^{-22} T_g}{P d^2} \quad (1)$$

where N, number of molecules per cubic meter; d, diameter of gas molecule; T_g, gas temperature; P, chamber pressure.

The influence of chamber pressure and gas temperature on the mean free path in the region of interest is illustrated in Fig. 1. It can be seen that the chamber pressure has great impact on the mean free path, i.e. the mean free path is changed tenfold in the pressure interval. It is also demonstrated that the influence of the gas temperature is only marginal. The gap between the shelf and the vial was in range of 0.05–0.6 mm and it would therefore be expected that the free molecule heat conduction regime would prevail at chamber pressures lower than approximately 10 Pa.

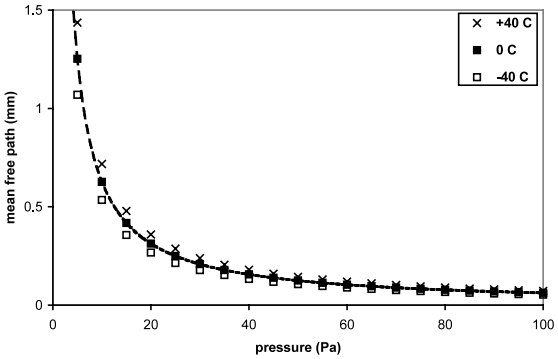

Fig. 1. Influence of chamber pressure and gas temperature on the mean free path.

Heat conduction at low pressures involves a mechanism of energy transfer by individual molecules incident on a surface. When molecules strike a surface complete interchange does not occur and the accommodation coefficient (α) is therefore introduced, which is a measure of the efficiency of energy exchange between the gas molecules and the solid surface:

$$\alpha = (E_r - E_i)/(E_s - E_i) \quad (2)$$

where E_r, energy brought to the solid surface in unit time by the incident gas molecules; E_i, energy carried away by the gas molecules after reflection; E_s, energy which the reflected molecules would carry away if it had the same mean energy as a gas in thermal equilibrium with the surface.

The following relation is valid for the accumulation coefficient if there is no accumulation of gas molecules at the solid surface and the energies are proportional to the corresponding surface or gas temperatures:

$$\alpha = (T_r - T_i)/(T_s - T_i) \quad (3)$$

where T_s, temperature of the shelf surface; T_i, temperature of the incident gas molecules; T_r, temperature of the reflected gas molecules.

The α-value will be 1 if the energy exchange is complete and the molecules assume the temperature of the surface and 0 if no exchange occur. In the system of interest two different solid surfaces occur, i.e. glass and stainless steel.

According to Demirel and Saxena (1996a) it is clear that the parameters, which can possibly influence α for engineering surfaces are: molecular weight of the gas and solid and temperatures of the gas and solid. Available data for α for a number of monoatomic, diatomic and polyatomic gases on different metal surfaces have been analyzed and the following correlation have been developed:

$$\alpha = F\left(\frac{M_g}{6.8 + M_g}\right) + (1 - F)\left(\frac{2.4\mu}{(1 + \mu)^2}\right) \quad (4)$$

where μ, ratio of molecular weights of gas to solid; F, fractional coverage of the adsorption layer which depends on the nature of the surface.

A general correlation for F would be:

$$F = \exp\left(\frac{C(T_r - 273)}{273}\right) \quad (5)$$

where C is a parameter related to the nature of the surface.

Demirel and Saxena (1996b) showed that $C = -2$ generated α-values that fitted different sets of α reported in literature for the system nitrogen–tungsten very well. Demirel and Saxena (1996a) showed that a $C = -0.7$ generated α-values that fitted experimental values of α for three monoatomic gases, He, Ne and Ar on Pt, Ni, Al, UO_2, Zr-2 and stainless steel surfaces. Fig. 2 shows calculated values of α for the two systems nitrogen-glass, i.e. N_2–SiO_2 and nitrogen–stainless steel, i.e. N_2–Fe, in the temperature interval of interest. It is demonstrated that α is very similar for the two systems and that C will only have a marginal influence on the values of α. It was decided to use $C = -2$ for both systems in the theoretical model because that value was found to be suitable for nitrogen at least in combination with tungsten. The significance of α in the simulation model was also evaluated.

Different theories for heat conduction in gases at low pressures have been developed. Knudsen developed a conduction theory for the free molecule regime (Dushmann and Lafferty, 1962). The energy transfer per unit area and unit time by molecular conductance between the vial and the shelf can according to this theory be described by the following expression under the assumption that the mean temperature of the gas will be equal to the mean temperature of the vial and shelf surface:

$$E = \alpha_m \Lambda_0 P \sqrt{\frac{273.2}{(T_s + T_v)/2}}(T_s - T_v) \quad (6)$$

where α_m is the mean accommodation coefficient for the system; Λ_0 is the free molecular conductivity for nitrogen at 0 °C; T_v is the temperature of the bottom surface of the vial.

The mean accommodation coefficient for the system was defined as:

$$\alpha_m = \frac{\alpha_{glass}\alpha_{ss}}{\alpha_{glass} + \alpha_{ss} - \alpha_{glass}\alpha_{ss}} \quad (7)$$

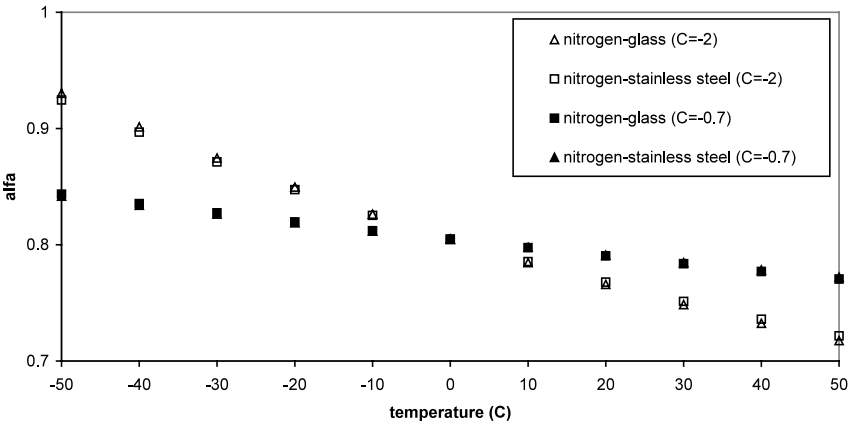

Fig. 2. Influence of temperature and value of C on the accommodation coefficient of nitrogen–glass and nitrogen–stainless steel.

where α_{glass} is the accommodation coefficient for nitrogen-glass (vial); α_{ss} is the accommodation coefficient for nitrogen-stainless steel (shelf).

Smoluchowski developed a heat conduction theory that is based upon the concept of temperature discontinuity. This theory can be seen as a development of the Knudsen theory to describe thermal conduction in the transition regime. It will give the following expression for the energy transfer per unit area and unit time:

$$E = \frac{(T_s - T_v)}{\frac{l}{k_m} + \frac{1}{\alpha_m \Lambda_0 P \sqrt{\frac{273.2}{(T_s + T_v)/2}}}} \quad (8)$$

where l is the gap between the vial and the shelf; k_m is the mean heat conductivity of nitrogen over the range T_s–T_v.

It was decided to use the Smoluchowski equation in the simulation model. It is seen that Eq. (8) approaches Eq. (6) as the gap width decreases.

The mean heat conductivity of nitrogen was derived from the following correlation (Dushmann and Lafferty, 1962):

$$k_m = 0.001\sqrt{T_s + T_v}\left(\frac{1 + 1.7 \times 10^{-5}(T_s + T_v) + 3.2 \times 10^{-8}(T_s + T_v)}{1 + 52/(T_s + T_v)}\right) \quad (9)$$

2.3. Thermal radiation

Heat radiation between real bodies is a complicated process, but fairly accurate results can often be obtained using simplifying assumptions. In this case the simplifying assumptions were that the surface of the vial and the shelf were opaque and parallel, that the areas exchanging radiation was of the same size, that radiation and absorption occurred in the same spectral range, that all radiation that left the shelf struck the vial and that absorption and radiation of intervening gases was negligible. The energy transfer per unit area and unit time by heat radiation between the surface of the vial and the shelf can then be shown to be (Bird et al., 1960):

$$Q = \sigma\left(\frac{1}{1 + (1/\varepsilon_{glass} - 1) + (1/\varepsilon_{ss} - 1)}\right) \times (T_s^4 - T_v^4) \quad (10)$$

where σ is the Stefan–Boltzmann constant; ε_{glass} is the thermal emissivity of glass; ε_{ss} is the thermal emissivity of stainless steel.

2.4. Equation of energy transport

It was assumed that the heat transfer within the vial only occurs through heat conduction. This assumption is further substantiated in Section 4. The vial was an axisymmetric container and the heat exchange with the surroundings was assumed to be axisymmetric. The modeled system was therefore described in two-dimensions with cylindrical coordinates. The equation of energy transport for each material in the system was expressed as:

$$Cp_V \frac{\partial T}{\partial t} = \frac{1}{r}\frac{\partial}{\partial r}\left(rk\frac{\partial T}{\partial r}\right) + \frac{\partial}{\partial z}\left(k\frac{\partial T}{\partial z}\right) \quad (11)$$

where Cp_v is the volumetric specific heat capacity ($=\rho Cp$); t is the time; r is the radial coordinate; z is the height coordinate; k is the heat conductivity.

The modeled system consisted of four different materials, the vial (glass), the content in the vial (water or ice) and the confined head space (air at atmospheric pressure). The values of the applied material constants are summarized in Table 1.

Table 1
Material constants

Material property	Units	Value
Cp_v (glass)	J m^{-3} K^{-1}	2.2×10^6
Cp_v (water)	J m^{-3} K^{-1}	4.2×10^6
Cp_v (ice)	J m^{-3} K^{-1}	2.0×10^6
Cp_v (air)	J m^{-3} K^{-1}	1.3×10^3
k (glass)	W m^{-1} K^{-1}	0.8
k (water)	W m^{-1} K^{-1}	0.6
k (ice)	W m^{-1} K^{-1}	2.1
k (air)	W m^{-1} K^{-1}	2.4×10^{-2}
α_m	–	0.5
ε_{glass}	–	0.9
ε_{ss}	–	0.9
Λ_0	W m^{-2} K^{-1} Pa^{-1}	1.3
d	m	3.7×10^{-10}
σ	W m^{-2} K^{-4}	5.7×10^{-8}
C	–	−2
μ (nitrogen/glass)	–	0.5
μ (nitrogen/stainless steel)	–	0.5
M (nitrogen)	g mol^{-1}	28

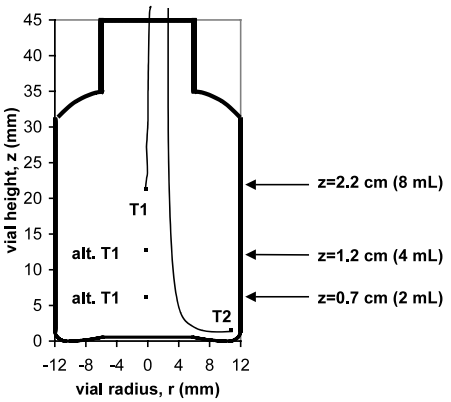

Fig. 3. A schematized cross-section of a 10-ml vial showing the position of the measuring points and the different fill heights in the study.

2.5. The design of the theoretical vial

The vial in the simulation model had the same design as the real vials from the bottom up to the vial shoulder (Fig. 3). The curvature of the bottom of the vial was described by polynomials fitted to experimental data (Fig. 4). The top of the vial was however simplified to a glass cylinder with the same diameter as the bottom of the vial. The height of the top cylinder was chosen so that the total weight of the vial would be equal to the real vials.

2.6. Numerical solution

The differential equation, Eq. (11), was coded for a numerical solution. The equation was discretized in both time and space using a finite difference method. A low-order time approximation called the backward difference method was used. It is unconditionally stable and results in a tridiagonal linear system of equations. The spatial finite difference equations were derived using the integration method described in Davis (1984). This method has the advantages that it is valid for non-uniform meshes and piecewise discontinuous equations. It was only necessary to model one vertical half of the vial due to axisymmetry.

The system of equations was solved using the following general initial and boundary conditions (Fig. 3).

At time $t = 0$, $T = T_0$.

For time $t > 0$,

$$-k\frac{\partial T}{\partial z} = 0 \qquad \text{at the top boundary } (z = 45 \text{ mm})$$

$$-k\frac{\partial T}{\partial r} = 0$$

at the right boundary ($r = 12$ mm) for vials in the center of the shelf

$$-k\frac{\partial T}{\partial r} = h(T_w - T_v)$$

at the right boundary ($r = 12$ mm) for vials in the corners of the shelf

where T_w, temperature of the walls of the freeze dryer.

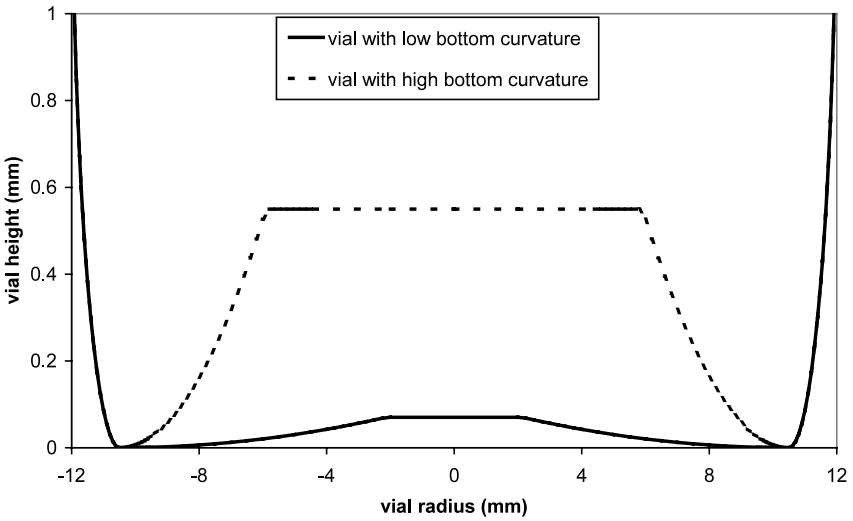

Fig. 4. A schematized cross-section of the outer surface of the bottom of one 10-ml vial with low bottom curvature and another with high bottom curvature.

$$-k\frac{\partial T}{\partial r}=0 \qquad \text{at the left boundary } (r=0 \text{ mm})$$

$$-k\frac{\partial T}{\partial z}=\frac{(T_s-T_v)}{\dfrac{l}{k_m}+\dfrac{1}{\alpha_m\Lambda_0 P\sqrt{\dfrac{273.2}{(T_s+T_v)/2}}}+\sigma\left(\dfrac{1}{1+(1/\varepsilon_{glass}-1)(1/\varepsilon_{ss}-1)}\right)\times(T_s^4-T_v^4)}$$

at the bottom boundary $(z=0 \text{ mm})$

3. Materials and methods

3.1. Materials

The experiments were carried out with 10 ml injection vials made of colorless borosilicate glass tubing of Ph. Eur. and USP type 1. The dimensions of the vials were according to size 10 R in ISO 8362-1. The vials were filled to different fill heights, i.e. 2, 4 or 8 ml, with distilled water. The vials were closed with FM 157 freeze-drying stoppers (Helvoet Pharma) and caps (West) after filling.

3.2. Freeze-dryer

The freeze-drying plant was manufactured by Edward Kniese & Co. The fully automated, programmable and steam sterilizable dryer had a condenser capacity of 11 kg and three temperature controlled shelves, each with a shelf area of 0.14 m^2. The distance between the shelves were 80 mm. The condenser was situated in a separate chamber, which was connected to the cabinet by a valve. The freeze-dryer was automatically controlled by a PLC (Siemens S5) that could be programmed from a connected PC. The condenser was cooled to about -80 °C while the temperature of the polished stainless steel shelves was varied between -45 and $+50$ °C. The temperature of the circulating silicone oil that controlled the temperature of the shelves was measured both at the inlet and at the outlet from the shelves. A platinum probe at the outlet regulated the shelf temperature. The operating pressure was regulated with a nitrogen injection through a micro valve and with the valve to the vacuum pump. The chamber pressure was measured with two different pirani manometers

(Edwards and Leybold) and a capacitive manometer (MKS Baratron). The capacitive manometer was used for the regulation and its operating range was 0.0001–1 mbar with an accuracy of ±0.5% of reading. Temperatures in the chamber were measured with 13 thermocouples of type K. The main part of these was mounted in vials but some were mounted on the shelf surface, on the upper or the bottom side, or on the chamber walls. Experimental data was logged on a PC and/or recorded on a printer.

3.3. Glass vial measurements

The exterior bottom curvature of the vial, thickness of the bottom wall, thickness of the sidewall, height, outer diameter and weight of vials from 10 different batches were measured. Ten vials were randomly chosen per batch, i.e. in total 100 vials. Exterior bottom curvature was measured on additional vials in order to sort out a total of 37 vials with exceptionally low curvature and just as many with exceptionally high curvature. The thickness measurement was performed with a Hall effect sensor, a Magna-Mike 8500 from Panametrics. The exterior bottom curvature was measured with a dial indicator mounted in a turning and boring machine.

Three vials were cut in two pieces at different heights, 0, 0.7 and 1.2 cm, which corresponded to the vial bottom and two different fill volumes (Fig. 3). The weight of the two pieces of each vial was measured.

3.4. Experimental design

The experiments were performed in such a way that the conditions for the heat transfer were the same as during a lyophilization process but without mass transfer or freezing taking place. A total of 215 vials were filled with distillated water and sealed with rubber stoppers and caps. The bottom curvature had been determined for 74 of these vials and half of these had high bottom curvature and the other half low curvature. Three vials with exceptionally low bottom curvature and just as many with high curvature were equipped with two thermocouples per vial. The thermocouples penetrated through the rubber stopper and the penetration point was reinforced with silicone rubber glue. The measuring point for one thermocouple was in the bottom corner (T2) and the other point was in the water surface in the center of the vial (T1) (Fig. 3). The vials were placed directly on the middle shelf in a hexagonal packing array. A shelf border in stainless steel surrounded the vials. The shelf above and beneath the vials was empty. All of the low curvature vials were placed in the center of one half of the shelf and the high curvature vials in the center of the other half. Each type of vial, i.e. low or high curvature, was tested at each of the halves of the shelf with the same process conditions. The monitored vials were either placed in the center or the corners of the shelf.

Five different chamber pressures, 5, 16, 30, 50 and 90 Pa and three different fill volumes, 2, 4 and 8 ml were tested. The vials were opened, emptied, dried, refilled and resealed when the fill volume was changed.

The shelf temperature was changed from the starting temperature to a set point temperature as fast as the freeze-dryer permitted. The shelf was kept at the set point until the vials reached a steady-state temperature that in most cases was the set point. The shelf was then changed back to the starting temperature and kept constant at that temperature until the vials reached the new equilibrium. Two different shelf temperature ranges were used in the experiments. The starting temperature and set point were +50 and −3 °C, respectively or −45 and −5 °C, respectively. That meant that the water in the vials were either liquid water or solid ice during the whole process.

4. Results and discussion

4.1. Vial measurements

The variations of the diameter and height of the 10-ml glass vials were small both within each batch and between the ten batches measured. The variations of the weight and the thickness were also small within each batch. There was however a significant difference in weight and glass thickness

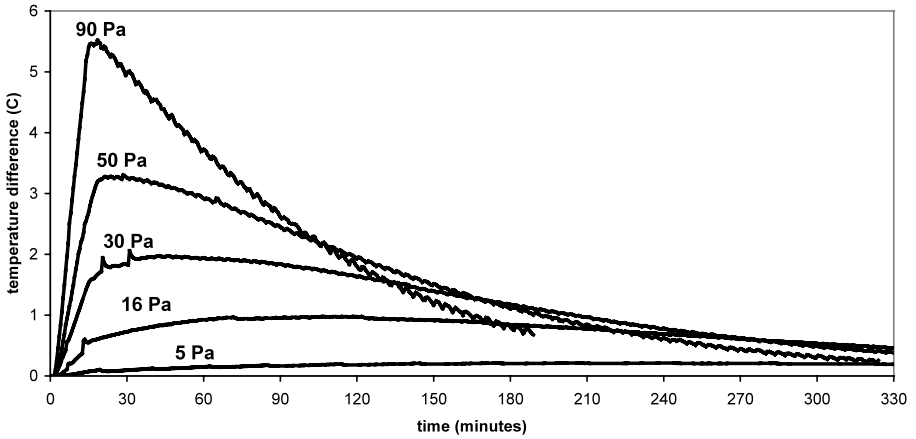

Fig. 5. Differences between the simulated temperatures of a vial with low bottom curvature and another vial with high curvature during cooling sequences at five different chamber pressures. The vials contained 8 ml of water and were situated in the center of the shelf.

between batches and an evident positive correlation between these parameters.

The weights of the different segments from the vials cut in two pieces at different heights correlated well with the corresponding theoretical geometries with a glass density of 2.6 kg/l.

Fig. 4 shows schematized bottom curvatures of a vial with low bottom curvature and another with high curvature. The difference in the gap to the shelf was approximately 0.5 mm between the different extreme vials. The average bottom curvature was approximately halfway between these extreme vials.

4.2. Influence of the bottom curvature of the vial

The influence of the bottom curvature of the vials was predicted with the simulation model and Fig. 5 shows predicted temperature differences between a low and a high curvature vial during cooling sequences at five different chamber pressures. It can be seen that the predicted maximum temperature difference between the extreme vials is small, lower than 1 °C, below 30 Pa, but significant, more than 2 °C, from that pressure and upwards. The theoretical maximum temperature difference was 5.5 °C between the two extreme vials at the highest pressure, 90 Pa. A similar pattern could be noticed experimentally but it was however not always consistent for all of the monitored vials. The vial-to-vial variation was found to be generally low, but it was larger for the high curvature vials than the low curvature vials. The precision of the experimental results was influenced by the precision in the temperature measurement and temperature variation across the shelf. The precision of the temperature measurements with the thermocouples was approximately ± 1 °C. The temperature variation across the shelf was found to be less than 1 °C. The combination of these two effects introduced an experimental variation large enough to partly have overshadowed the effect of the bottom curvature.

4.3. Influence of the state of the water in the vials

Fig. 6 shows monitored temperatures and corresponding simulated temperatures for a vial containing ice during a heating and cooling sequence and Fig. 7 shows the same for a vial containing water. It can be seen in both figures that the heating and cooling behavior is equivalent. The temperature response in the vial generated by the change in shelf temperature reflects the resistance of the heat transfer to the vial and the accumulation of heat in the vial. It is well demonstrated in both figures that the simulated result and the experimental data corresponds well and that the dynamics of the system is well modeled. Both the time it takes to warm or cool

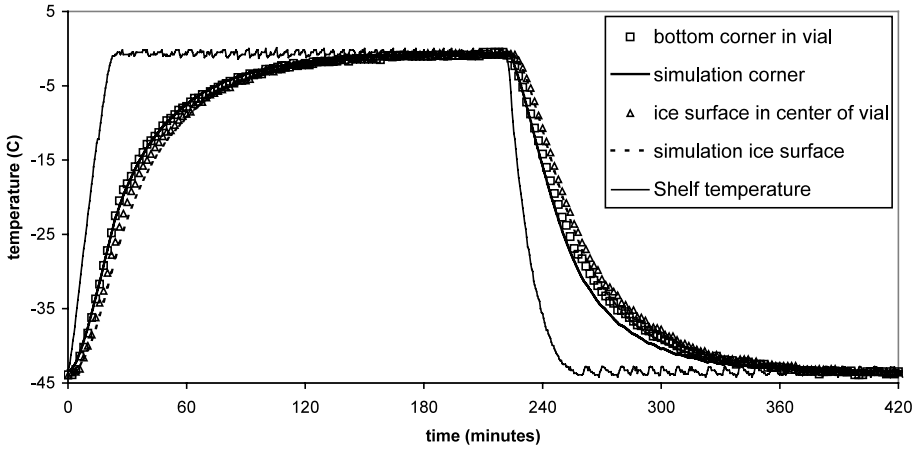

Fig. 6. Monitored and corresponding simulated temperatures of a low curvature vial in the center of the shelf containing 8 ml of ice during a cooling and heating sequence at 50 Pa. Both monitored positions in the vial are illustrated, the one in the bottom corner and the other in the ice surface in the center of the vial.

the vial and the temperature difference between the different positions in the vial is well simulated.

It can be seen in Fig. 7 that the experimental data indicates a somewhat different behavior during heating of the vial containing water than during cooling. The mean temperature difference between the two positions in the vial was approximately 4 °C smaller during the heating than during the cooling sequence. This difference could not be detected in the simulation or in the experiments with ice. It was probably an effect of free convection of the water when it was heated from below. The theoretical model is based on an assumption that there is only heat conduction in the material in the vial and the simulation does therefore not take the free convection effect into account. This effect can however be neglected for vial lyophilization since it did not appear during cooling and the content in the vial will after the freezing stage be a frozen solution or a semidry solid.

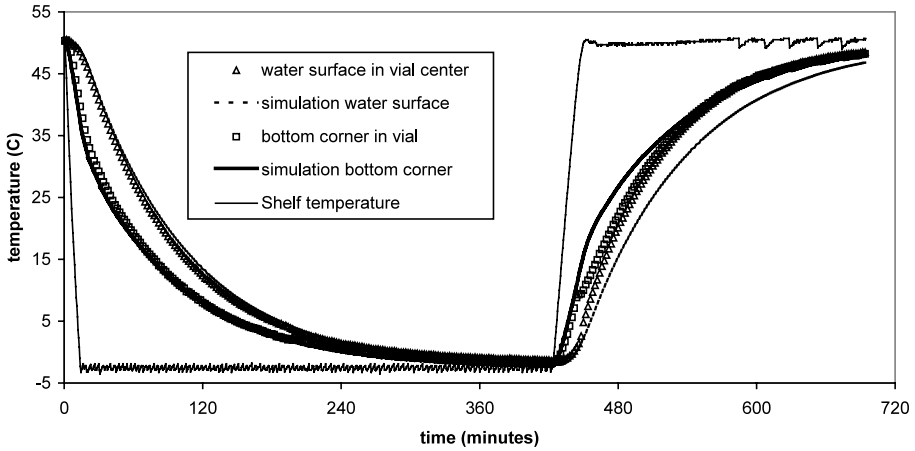

Fig. 7. Monitored and corresponding simulated temperatures of a low curvature vial in the center of the shelf containing 8 ml of water during a cooling and heating sequence at 30 Pa. Both monitored positions in the vial are illustrated, the one in the bottom corner and the other in the water surface in the center of the vial.

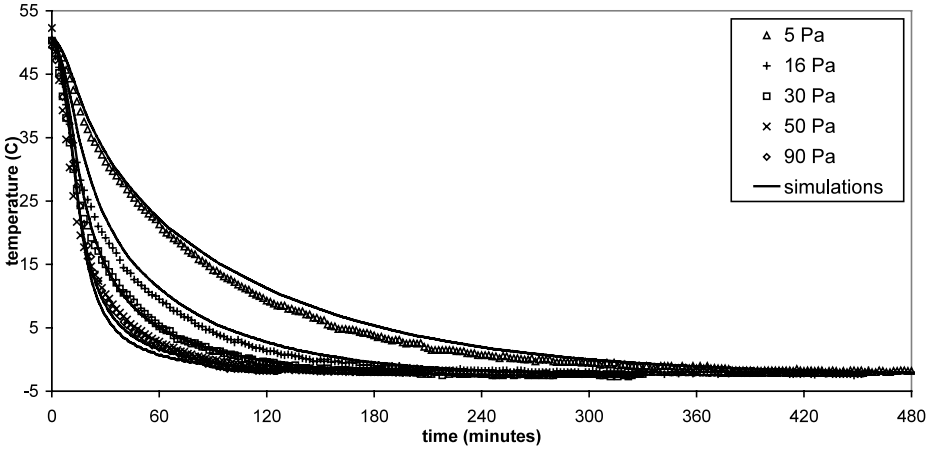

Fig. 8. Monitored and corresponding simulated temperatures of the bottom corner of a low curvature vial in the center of the shelf containing 2 ml of water during a cooling sequence at five different chamber pressures.

4.4. Influence of fill volume and chamber pressure

Figs. 8, 9 and 10 show monitored and corresponding simulated temperatures during a cooling sequence of vials with different fill volumes and applied chamber pressures. It can also here be seen that the simulated and experimental data corresponds well and that the influence of fill volume and chamber pressure is well modeled. The influence of the fill volume was relatively small and this is probably due to the fact that the heat capacity of the glass vial has a dominating effect.

4.5. Influence of the position on the shelf

Table 2 shows monitored temperatures in the center and in the corner of the shelf at the end of the cooling sequence. The vial in the corner did not reach the shelf temperature and the temperature was 3.5–8.5 °C higher than the shelf temperature. The temperature gradient across the shelf was monitored and found to be very low, less than 1 °C, and it can therefore not explain the obtained difference in temperature. The vial in the corner must have received a significant amount of heat

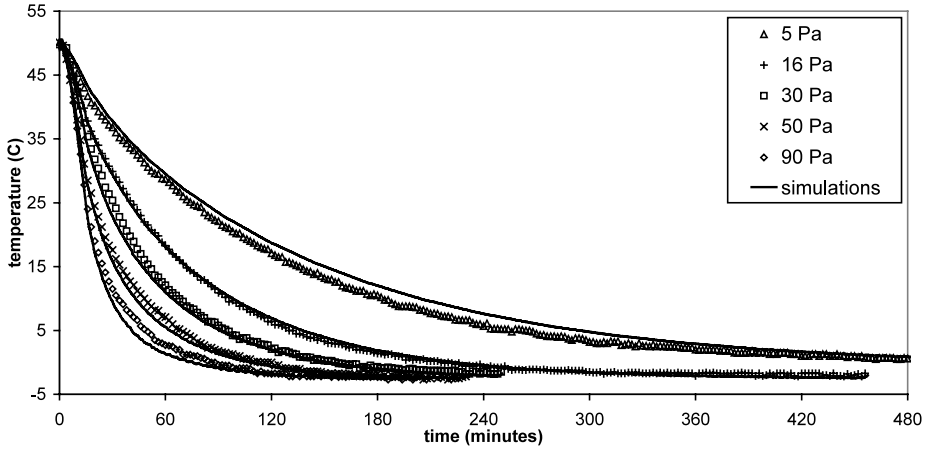

Fig. 9. Monitored and corresponding simulated temperatures of the bottom corner of a low curvature vial in the center of the shelf containing 4 ml of water during a cooling sequence at five different chamber pressures.

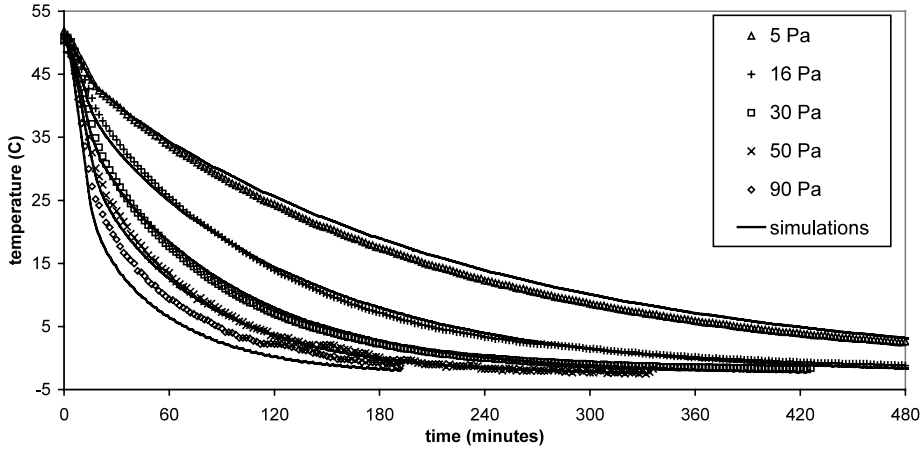

Fig. 10. Monitored and corresponding simulated temperatures of the bottom corner of a low curvature vial in the center of the shelf containing 8 ml of water during a cooling sequence at five different chamber pressures.

Table 2
Monitored temperatures at different positions on the shelf at the end of the cooling sequence when the mean shelf temperature was −43.5 °C

Chamber pressure (Pa)	Position on the shelf	Mean temperature in bottom of the vial (°C)
5	Center	−42.5
	Corner	−35
16	Center	−43.5
	Corner	−38
50	Center	−43.5
	Corner	−40

The vials contained 2 ml of ice.

from another source than the shelf. The temperature difference between the vial and the shelf decreased with increasing chamber pressure, which must be due to the fact that the heat transfer from the shelf increases more with pressure than the heat transfer from the other sources. It was assumed that heat was exchanged between the walls of the freeze-dryer and the corner vials and that it was evenly and axisymmetrically distributed along the side of the vial. The temperature of the walls of the freeze-dryer was monitored and found to be constantly at approximately 15 °C during the whole process and this temperature was used in the simulations. The amount of heat exchange with the walls and the corresponding heat transfer coefficient were evaluated from the experimentally determined temperature differences between the shelf and the corner vials at the end of the cooling sequence.

The vials in the center of the shelf were completely surrounded by neighbors in a hexagonal array and were therefore well shielded. There was therefore no temperature difference between the shelf and the center vials except at the lowest pressure where the temperature of the vials was slightly higher than the shelf. The effect of other heat sources can therefore be neglected in the center of the shelf except at the lowest pressure where a marginal effect can be expected.

Fig. 11 shows monitored temperatures and corresponding simulated temperatures for a vial in the center and another in the corner of the shelf during a heating and cooling sequence. It is demonstrated that the dynamics of both vials are well modeled.

4.6. Influence of the mean accommodation coefficient

The influence of α_m was investigated by changing it ± 0.1 units and determining the effect on the simulated results. The chosen variation corresponded to an increase of α_m of 12% and a decrease of 18%. This seemed reasonably large considering that a change of the constant C from

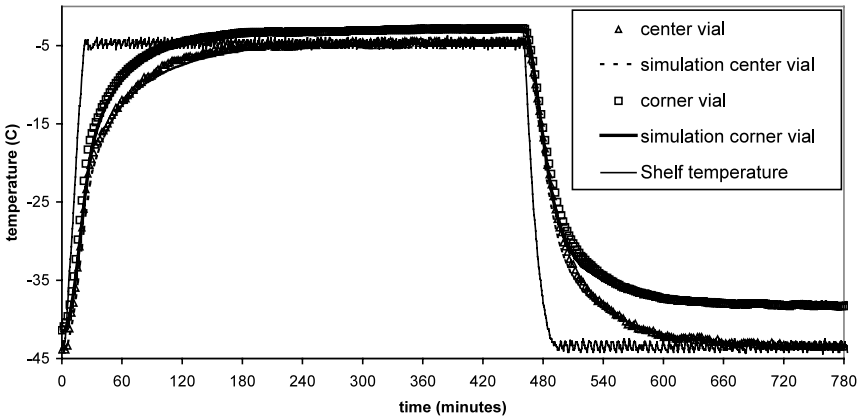

Fig. 11. Monitored and corresponding simulated temperatures of a low curvature vial in the center of the shelf and another low curvature vial in the corner of the shelf during a cooling and heating sequence at 16 Pa. The vials contained 2 ml of ice.

-2 to -0.7 for both α_{glass} (N_2–glass) and α_{ss} (N_2–stainless steel) would result in a 12% increase of α_m at 50 °C, a 18% decrease at -50 °C and no change at 0 °C. These two values of C have been reported in Demirel and Saxena (1996a,b) to fit several gas–solid systems including nitrogen and stainless steel although not the combination of these two. The chosen variation of α_m was therefore considered to reflect the expected uncertainty. The maximum temperature difference between the simulation with the lowest and the highest α_m was approximately 4 °C. This is slightly lower than the theoretical influence of the bottom curvature. The influence of α_m on the simulation model was therefore considered to be moderate provided that the equations for α for the two gas–solid systems are reasonably correct.

4.7. Influence of the glass vial

Fig. 12 shows simulated temperature profiles at six different times during a cooling sequence of a vial containing 2 ml of water. It can be seen that the top of the glass vial is lagging relative to the content in the vial. The lag effect is due to a combination of the heat transfer resistance of the thin glass walls and the heat capacity of the relatively large glass top. The temperature difference between the top and the bottom of the vial therefore becomes considerable during the first part of the heating sequence. It is also illustrated that the temperature profile in the water will be curved towards the water surface in the center of the vial. The curved profile is formed because of the influence of the bottom curvature and the heat accumulation in the glass vial above the water surface. The curvature will however decrease with increasing fill volume.

Fig. 13 demonstrates the dynamic effect of the glass vial itself. It takes about four times as long time to reach the steady-state temperature when the vial is included in the simulation and the total time for the heating sequence is significant, i.e. about 4 h. It is therefore clear that the effect of the heat accumulation in the vial is important. Numerically, the heat accumulation in the vial was excluded by reducing the heat capacity of the glass by a factor of 100 000. The effect of the vial depends on the fill volume and it becomes dominating at low coefficients of fullness. It is common to use a low coefficient of fullness for pharmaceuticals lyophilized in vials in order to achieve a reasonable drying time and a fill volume of 2 ml in a 10-ml vial could be a likely choice. It can therefore be concluded that the dynamics of the vial should not be neglected.

4.8. Relative importance of different heat transfer modes

The theoretical model for the heat transfer between the shelf and the vial included both heat

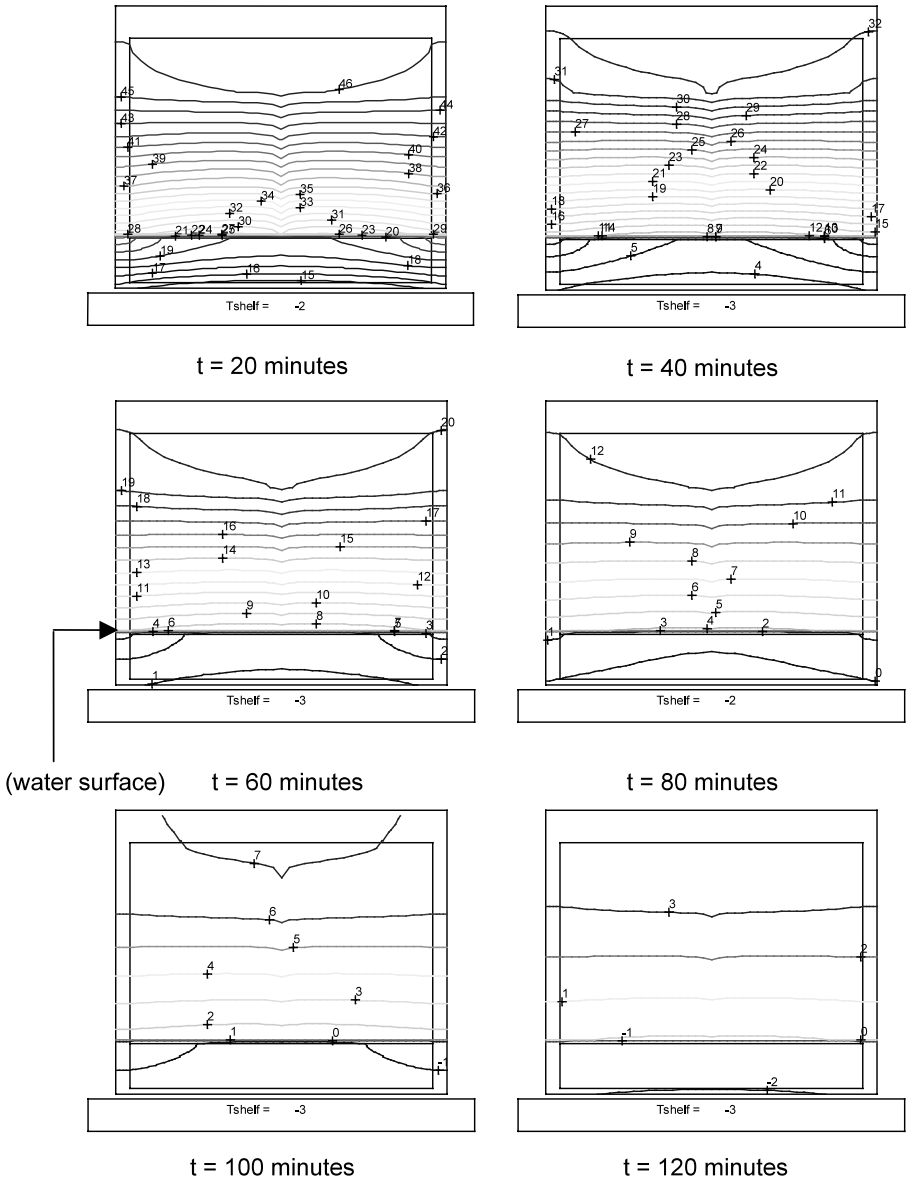

Fig. 12. Simulated temperature profiles at six different times, during a cooling sequence at 90 Pa of a low curvature vial in the center of the shelf containing 2 ml of water.

radiation and heat conduction through the gas between the shelf and the vial. It is possible from the simulation model to calculate the influence of the two different heat transfer modes. Fig. 14 illustrates the relative importance of the heat radiation at different chamber pressures. It also demonstrates the influence of the chamber pressure on the overall heat transfer coefficient. The relative importance of the heat radiation reduces logarithmically with increasing chamber pressure while the overall heat transfer coefficient increases proportionally with chamber pressure. Heat radia-

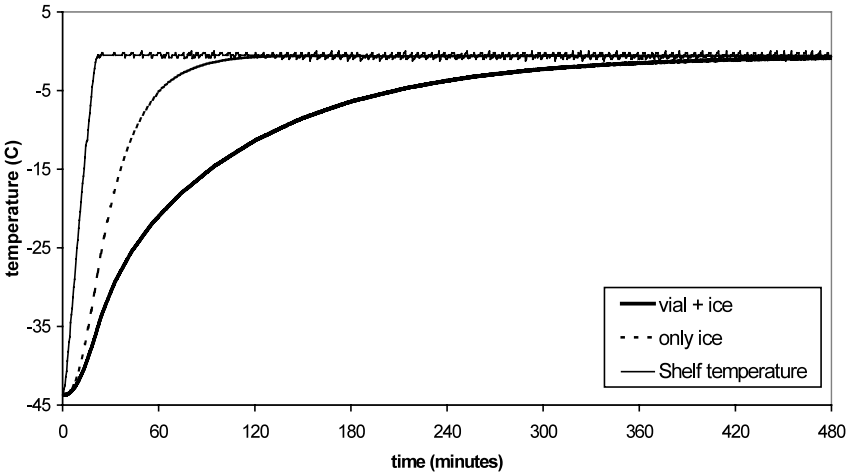

Fig. 13. Simulated temperatures of the bottom corner of a low curvature vial containing 2 ml of ice during a heating sequence at 5 Pa.

tion dominates at the lowest pressure whereas heat conduction dominates at pressures from 16 Pa and upwards. The relative importance of the heat radiation was lower for the experiments performed at low shelf temperatures with ice. The overall heat transfer coefficients were however approximately the same because the lower thermal radiation was compensated by a higher thermal conduction in the gas due to an increase of the accommodation coefficients.

5. Conclusions

The dynamic two-dimensional theoretical model could well describe the cooling and heating of the vials and there was a good agreement between simulated and experimental data. Both the heat transfer between the vial and the shelf and the heat accumulation in the vial were therefore well modeled. Also the dynamics of the corner vials could be well modeled by adding heat exchange

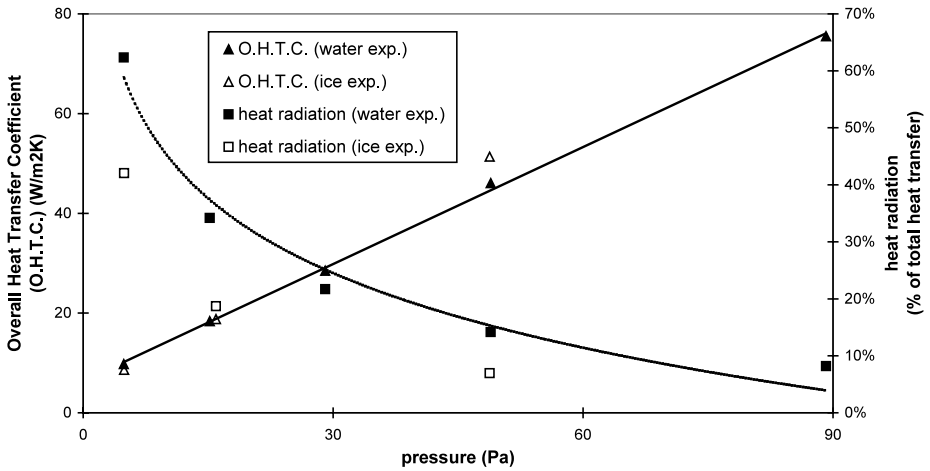

Fig. 14. Predicted influence of chamber pressure on the Overall Heat Transfer Coefficient (O.H.T.C.) and relative importance of heat radiation. The figure shows predictions for experiments at low shelf temperatures (−45 to −5 °C) with ice and at high shelf temperatures (+50 to −3 °C) with water.

between the walls in the freeze-dryer and the side of the vial. The value of the heat transfer coefficient for this heat exchange was however determined from experimental data and not based on theoretical relations only as in the original model.

The theoretical model can be used to predict and better understand the dynamics of heat transfer in vial lyophilization. One thing that could be concluded was that heat accumulation in the glass vial would have significant influence on the heating and cooling dynamics at low coefficients of fullness of the vial and that should not be neglected in vial lyophilization. Another conclusion was that the relative importance of heat radiation reduces logarithmically with increasing chamber pressure while the overall heat transfer coefficient increases proportionally with increasing chamber pressure. Heat conduction through the gas between the shelf and the vial was the dominating heat transfer mechanism except at the lowest pressure, 5 Pa, where heat radiation dominated.

The effect of the bottom curvature of the vials on the heat transfer was pressure dependent. It was insignificant at the lowest pressure but increased with increasing pressure.

Heat exchange from other sources than the shelf could be neglected for vials in the center of the shelf but not for vials in the corner, which lacked neighboring vials and therefore were unshielded from the surroundings.

This study has shown that it is necessary to use a two-dimensional simulation model in order to describe the system adequately. The effect of the curvature of the vial bottom, the heat accumulation in the glass vial and the heat transfer to the sidewalls of vials in the corner of the shelf all contributed to a significant radial influence on the heat transfer.

The developed simulation model will serve as a good fundament for the further development of a theoretical model for vial lyophilization.

References

Bird, R.B., Stewart, W.E., Lightfoot, E.N., 1960. Transport Phenomena. Wiley, p. 445.

Davis, M.E., 1984. Numerical Methods and Modeling for Chemical Engineers. Wiley, pp. 185–190.

Demirel, Y., Saxena, S.C., 1996. Heat transfer through a low-pressure gas enclosure as a thermal insulator: design considerations. International Journal of Energy Research 20, 327–338.

Demirel, Y., Saxena, S.C., 1996. Heat transfer in rarefied gas at a gas–solid interface. Energy 21, 99–103.

Dushmann, S., Lafferty, J.M., 1962. In: Lafferty, J.M. (Ed.), Scientific Foundations of Vacuum Technique. Wiley, p. 28–30, 45–51.

Mascarenhas, W.J., Akay, H.U., Pikal, M.J., 1997. A computational model for finite element analysis of the freeze-drying process. Computer Methods in Applied Mechanics and Engineering 148, 105–124.

Pikal, M.J., 1985. Use of laboratory data in freeze drying process design: heat and mass transfer coefficients and the computer simulation of freeze drying. Journal of Parenteral Science and Technology 39, 115–139.

Pikal, M.J., Roy, M.L., Shah, S., 1984. Mass and heat transfer in vial freeze-drying of pharmaceuticals: role of the vial. Journal of Pharmaceutical Sciences 73, 1224–1237.

Pikal, M.J., Shah, S., Senior, S., Lang, J.E., 1983. Physical chemistry of freeze-drying: measurement of sublimation rates for frozen aqueous solutions by a microbalance technique. Journal of Pharmaceutical Sciences 72, 635–650.

Rene, F., Wolff, E., Rodolphe, F., 1993. Vacuum freeze-drying of a liquid in a vial: determination of heat and mass-transfer coefficients and optimisation of operating pressure. Chemical Engineering and Processing 32, 245–251.

Schoen, M.P., Braxton, B.K., Gatlin, L.A., Jefferis, R.P., III, 1995. A simulation model for the primary drying phase of the freeze-drying cycle. International Journal of Pharmaceutics 114, 159–170.

Sheehan, P., Liapis, A.I., 1998. Modeling of the primary and secondary drying stages of the freeze drying of pharmaceutical products in vials—numerical results obtained from the solution of a dynamic and spatially multi-dimensional lyophilization model for different operational policies. Biotechnology and Bioengineering 60, 712–728.

Ybema, H., Kolkman-Roodbeen, L., Te Booy, M.P.W., Vromans, H., 1995. Vial lyophilization: calculations on rate limitation during primary drying. Pharmaceutical Research 12, 1260–1263.